

# Coherent Radiometers for Cosmic Microwave Background Polarization Detection

Todd C. Gaier  
Jet Propulsion Laboratory, California Institute of Technology

## ABSTRACT

Coherent radiometers have been used for decades in the detection of polarization of astronomical signals. Recent success in detection of intensity fluctuations of the Cosmic Microwave Background (CMB) has created great interest in the potential measurement of CMB polarization. Detection of polarization at predicted levels may stretch the sensitivity of today's radiometers. I will review the state-of-the-art of receiver front-ends, discuss their application to polarimeter design in experiments, both existing and under development and finally describe the prospects for massive arrays for the detection of CMB polarization.

## 1. INTRODUCTION

The study of the anisotropy of the cosmic microwave background (CMB) has proven to be an enormously rich and successful scientific endeavor, yielding such basic information as the density and age of the Universe, the primordial fluctuation spectrum and the energy of empty space Refs [1,2,3,4]. This recent success has been fueled by the development of ultra-low noise receivers operating in arrays, both filled aperture focal plane and interferometers..

The detailed mapping of intensity fluctuations of the CMB has enjoyed great success with detection by COBE at large angles, followed by small maps on smaller scales by the South Pole, Saskatoon, and MAXIMA experiments and then detailed high resolution maps on larger portions of the sky by BOOMERANG, CBI and DASI. The CMB intensity fluctuations will be mapped full sky at high resolution by MAP and later by Planck. These results and the prospect of expanding the science horizons of CMB study have re-ignited the interest in CMB polarization. The CMB has intrinsic intensity fluctuations of approximately 100  $\mu\text{K}$  at sub-degree pixel size. The signal is expected to have a polarization fraction of nearly 10%, but as of today detection of CMB polarization has not been published. The current best upper limits to the polarization are 8 $\mu\text{K}$  at sub-degree scales Ref [5].

With recent reconfiguration of the DASI experiment at the South Pole and the successful launch of MAP, it is likely that E-mode polarization (curl-free) will soon be detected soon. The most compelling science comes from the so called, B-mode polarization (curl component), which may trace gravity waves in the early Universe Ref[6]. The level of B-mode polarization is likely to be at least an order of magnitude smaller than E-mode, forcing scientists to carefully evaluate receiver design and sensitivity to determine the feasibility of an experiment, which might make a detailed measurement of B-mode fluctuations. While coherent detection of broadband radiation is inherently less sensitive than incoherent detection, it offers unique advantages for polarization study as well as adequate sensitivity for ground-based measurements, where atmospheric noise can dominate.

## 2. COHERENT RECEIVERS

### 2.1 Coherent Detection

Coherent detection of radiation is fundamentally different than incoherent detection. With coherent detection, the incoming electric field signal is amplified coherently, processed to separate signal from spurious noise, and detected. The process of amplification, maintaining the incoming waveform, is

inherently noisy, limited by quantum mechanics Ref[7], so that the signal has a minimum added noise given approximately by:

$$T_q \geq h\nu/k_B \quad [1]$$

Where  $T_q$  is the quantum noise temperature,  $h$  is Planck's constant,  $k_B$  is Boltzmann's constant and  $\nu$  is the frequency of the incoming wave.

The very best receiver front-ends have noise a few times the quantum limit. The state-of-the-art in cryogenic coherent receiver noise from 10-400 GHz, the frequencies of interest for CMB measurements, is shown in Figure 1. The two technologies contributing the best practical results are cooled InP High Electron Mobility Transistor (HEMT) amplifiers, at frequencies up to 100 GHz and Superconductor-Insulator-Superconductor (SIS) mixers up to 400 GHz. The typical performance over this range is 3-5 times  $T_q$ . At 8 GHz an amplifier has been built by Chalmers Institute, using TRW/JPL InP HEMTs, yielding a noise of 1.5K or 3 times quantum limited noise, when cooled to 20 K Refs[8,9].

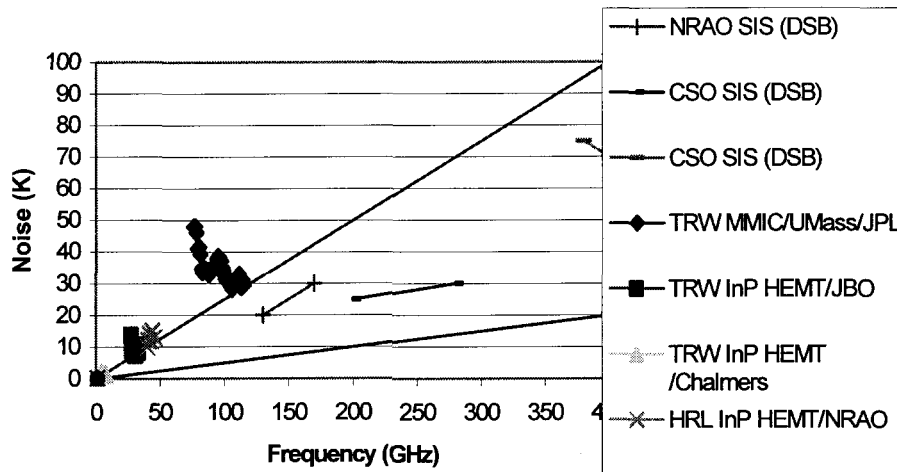


Figure 1. The state-of-the-art in receiver noise performance. Mixer performance is given as a double-sideband performance, relevant for continuum measurements.

The coherent receivers with either front end element require additional amplification in order to detect the small astronomical signals. While amplifiers have very good high frequency noise, they suffer from gain fluctuations with a  $1/f$  noise spectrum. The minimum detectable temperature signal from a radiometer in a time  $\tau$ , is given by Refs[10]:

$$\Delta T = (T_{sys} + T_{source}) \left[ \frac{1}{\beta\tau} + \left( \frac{\Delta G(\tau)}{G} \right)^2 \right]^{1/2} \quad [2]$$

where  $T_{sys}$  is the receiver noise temperature,  $T_{source}$  is the Rayleigh-Jeans temperature of the observed target and  $\beta$  is the detected bandwidth. The second term in the brackets is the normalized gain fluctuation in a time  $\tau$ , given by the properly normalized integral of the power spectrum of gain fluctuations. Most microwave amplifiers exhibit gain fluctuations of the form  $\Delta G(\nu)/G \propto \nu^{-1/2}$  or  $1/f$  in power. This limitation on the low frequency stability forces the receiver to stabilize the signal in other ways.

The most basic technique employed to stabilize radiometers was developed by Dicke Ref[11] and involves comparing the signal with a reference.

## 2.2 Coherent receiver designs for CMB measurement

Typical receiver noises for CMB measurement are in the tens of kelvins. The CMB temperature is 2.725 K and the fluctuations are more than 4 orders of magnitude below that. This requires measurements with wide bandwidth and long integration times.

The total power Dicke radiometer, shown in Figure 2, modulates the input to the radiometer between a signal and a reference. If the difference in amplitude between the signal and the reference is small, the output is stable. For a reference which contains no useful information, the resulting noise is given by the first term in Eq. 2, with a penalty of a factor of two. If two points on the sky are used, both with signal, the output is the difference and a  $\sqrt{2}$  penalty is paid (if the source is a random field, there is no penalty, since the signal grows by  $\sqrt{2}$ ). If the entire scan of many pixels can be carried out in a time where the gain fluctuation is small, no penalty is paid. This is the type of receiver used by COBE-DMR, the South Pole '94 and Saskatoon experiments. It is also the same type of receiver used by Lubin and Smoot

for a polarization measurement Ref[12]. This type of receiver does not take advantage of the coherent nature of the receiver.

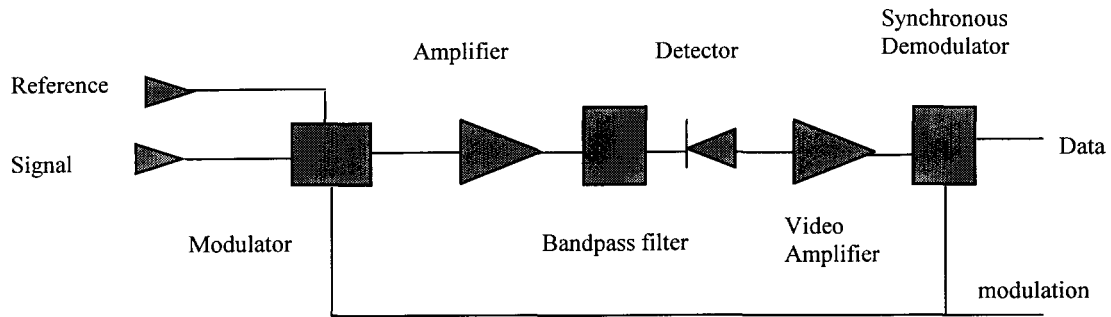


Figure 2. Schematic diagram of a Dicke-switched receiver.

The correlation receiver passes a signal and a reference wave through the same amplification chain. The coherent signals are separated later, detected and differenced. The common gain path ensures gain fluctuation reduction (for small signal and reference asymmetry). A variation of this, the pseudocorrelation receiver has been used by MAP, Planck-LFI as well as polarization experiments POLAR, PIQUE and COMPASS. In the MAP and Planck designs, the signal is passed through a hybrid coupler (Figure 3), amplified, phase switched in one leg, passed through a second hybrid. In MAP the signal is increased with a amplifier prior to the second hybrid band defined and detected. In Planck, the additional amplification and band definition are applied after the hybrid. If the noise penalty of this type of receiver is  $\sqrt{2}$  better than the Dicke receiver, but there are twice as many amplifiers. The systematics of this type of receiver are described in detail in Seiffert et al. Ref [13]. This design will be discussed later as the basis for a polarimeter.

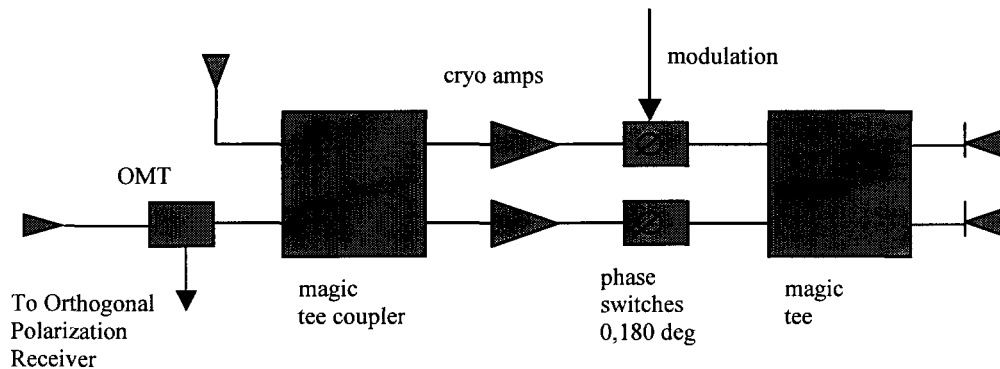


Figure 3. Schematic for a pseudocorrelation receiver as used by MAP and Planck-LFI. The magic tee coupler produce the sum and difference of the two inputs (divided by  $\sqrt{2}$ ). Band definition filters have been omitted for simplicity.

In a related idea, the receivers may be configured in an interferometer. In this case multiple receivers are pointed, with their own antennae, at the same part of the sky. The amplified outputs are then correlated (or multiplied and detected). The response to the telescope then depends upon the relative phase lags of the incoming signals, which is a function of the receiver spacing and antenna pattern. The response pattern or *visibility function*, of the interferometer is the windowed Fourier transform of the sky brightness distribution Ref [10]. Again, because the coherent input signal, and reference (in this case the average sky temperature across the whole field) has passed through the same gain paths, the  $1/f$  noise is reduced. Many telescopes use interferometry today and the VLA, CBI, the VSA and DASI have used this technique for CMB research.

### 2.3 Polarimeter Designs

An arbitrary wave coming from the sky received at an aperture plane can be written as:

$$\mathbf{E} = \mathbf{E}_x(t) + \mathbf{E}_y(t)$$

Where  $E_x(t)$  and  $E_y(t)$  are the time varying fields (both slow and fast) in the horizontal or x and vertical or y directions respectively. This becomes the basis for which we may evaluate polarimeters. Let  $E_x(t) = h(t)x \sin(\omega t + \delta_x(t))$  and  $E_y(t) = v(t)y \sin(\omega t + \delta_y(t))$  then  $H = h^2 / Z$  and  $V = v^2 / Z$  is the instantaneous power in each polarization, where  $Z$  is the impedance of the medium. The Stokes parameter  $I$  is given by  $H + V$ . Note that by this definition,  $I = (1/2)(T_x + T_y) k\beta$ , which is twice value typically used for the intensity fluctuation measurement of the CMB.

The Dicke radiometer has been adapted to polarimetry by using a polarization modulator in the front-end Ref[12]. The common version of this is a Faraday rotation polarizer. The output of the polarizer is either h or v depending upon sign of the magnetic field applied to the polarizer. The signal is then amplified, filtered and detected. By switching the field rapidly, and synchronously demodulating the signal, the receiver measures  $H - V$  (normalized to the input), which is the Q Stokes parameter. The noise is given by  $\Delta Q = T / \sqrt{\beta\tau}$ .

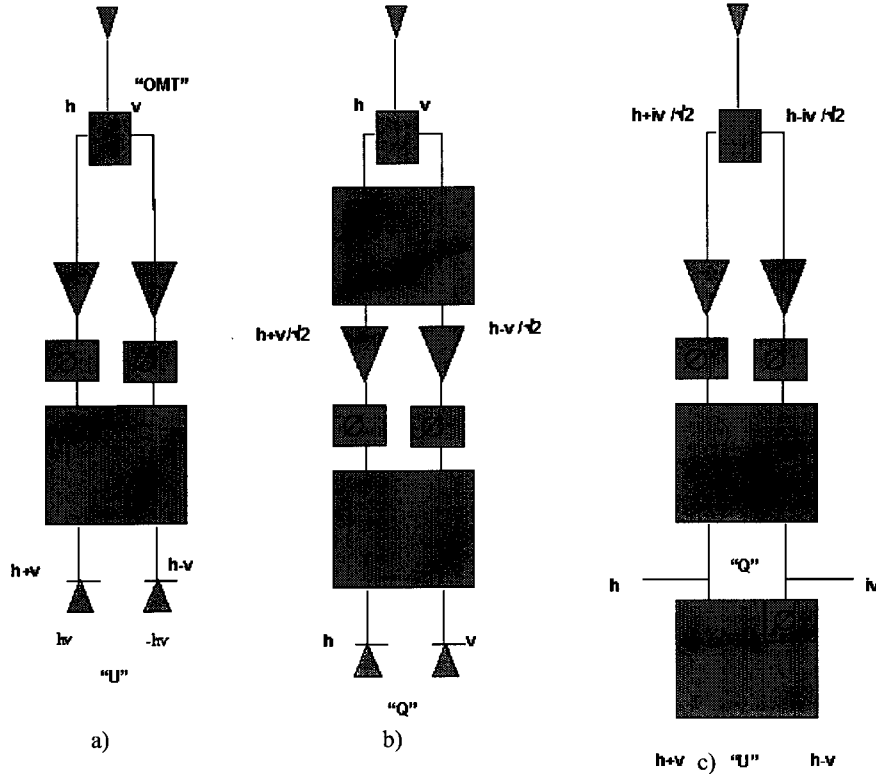


Figure 4. a) Shows the schematic of the POLAR and PIQUE polarimeters, with the multiplier function shown as a hybrid with two diodes. b) Shows the schematic of the COMPASS polarimeter. c) Shows a polarimeter design capable of detecting Q and U, using a circular polarization OMT.

A different design for a polarimeter was used in the POLAR and PIQUE experiments. These experiments used an orthomode transducer (OMT), at the base of a feed horn. The OMT passes h and v at its output ports. Each of the signals is amplified and multiplied (see Figure 4a). A phase switch is used to remove offsets and gain fluctuations after detection. In both of these experiments the signal is mixed down after amplification and then multiplied. Phase modulation is applied to the local oscillator of the mixer, providing a broadband, amplitude and phase matched response in the two states Refs[14,5]. The multiplier serves the function  $h \cdot v$ . If h and v are uncorrelated, the output is 0. If h and v are correlated and equal amplitude and phase, the demodulated output is  $2hv$  which (again, normalized to the input) is the U Stokes parameter. The noise is given by  $\Delta U = T / \sqrt{2\beta\tau}$ . The V Stokes parameter will not be considered since it is not an expected signal (but it is 0 anyway). The radiometer has no sensitivity to Q. Intensity signals I, if passed, do not receive systematic rejection of gain fluctuations.

Another polarimeter design uses the pseudocorrelation design of MAP and Planck. The COMPASS design uses an OMT, with the h and v signals passed into a hybrid (Figure 4b). The signals  $h+v/\sqrt{2}$  and  $h-v/\sqrt{2}$  are then amplified and one leg synchronously phase shifted. The signals are then passed into a second hybrid with the outputs h and v. They are then band defined, detected and synchronously demodulated. The output is thus H-V or Q. The noise is also  $\Delta Q=T/\sqrt{2}\beta\tau$ . If h and v are correlated and in phase, the signal only passes through one amplification chain, so although this design appears to offer potential sensitivity to U, it offers no systematic rejection.

Now we will consider the polarimeter which simultaneously detects Q and U. The design uses an OMT with outputs corresponding to the *two circular polarizations*. In this case one output is  $(h+iv)/\sqrt{2}$  and the other is  $(h-iv)/\sqrt{2}$  (Figure 4c). Both signals are then amplified and a synchronous phase switch applied one leg. The signals are then passed to a hybrid coupler with outputs h and iv, upon detection and synchronous demodulation these become H-V or Q with the noise given by  $\Delta Q=T/\sqrt{2}\beta\tau$ . Signal which is purely linearly polarized h or v, passes through all amplifiers. A  $45^\circ$  linearly polarized (pure U) also passes through both amplification chains. One only need tap off the h and iv signals, phase lag and multiply (with an additional synchronous phase shift) to get the output U. This output will have a noise  $\Delta U=T/\sqrt{2}\beta\tau$ . Since Q and U are equivalent upon a  $45^\circ$  rotation, this radiometer serves the function of two receivers which detect only Q or U, where both Stokes parameters are required. This radiometer topology has been proposed by the SPORt and Bar-SPORt team Ref[15,16].

It is worthwhile to discuss MAP and Planck-LFI as polarimeters. On MAP the pseudocorrelation receivers have two inputs looking at two different positions on the sky, through orthogonal polarizations of orthomode transducers. The instrument is not fundamentally a polarimeter, but will make polarized maps with some systematic rejection due to the cross-polar nature of the input signals (although the details of the polarization reconstruction are not known to the author)Ref [17]. Each receiver of Planck will make a map of the entire sky in a single polarization. Each horn will also receive the orthogonal polarization, and the focal plane arranged to provide maximum Q and U coverage. The ultimate fidelity of the polarization maps of MAP and Planck, is only as good as the intensity maps.

### 3. MMIC AMPLIFIERS AND INTEGRATED MODULES

#### 3.1 MMIC Amplifiers

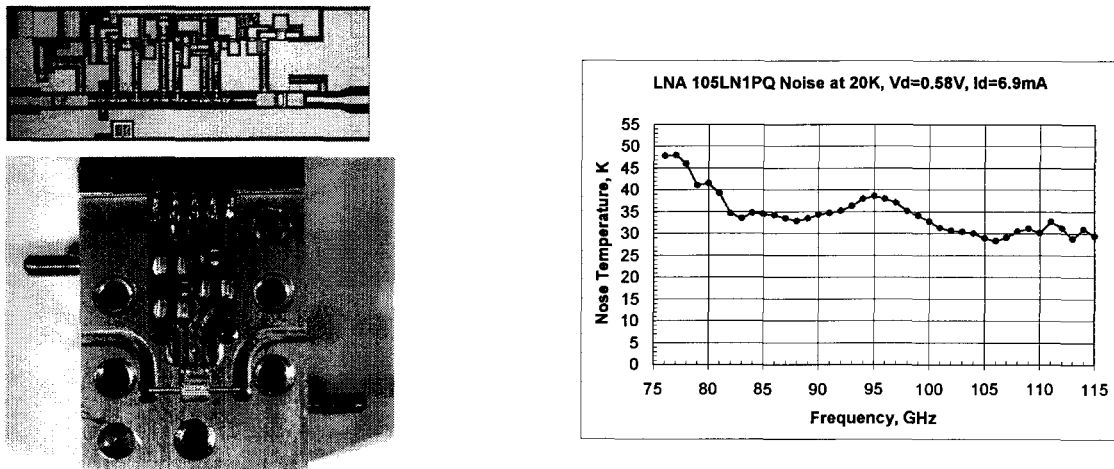


Figure 5. This figure shows a photograph of the 70-110 GHz MMIC amplifier chip, with size 2100x850 microns. The chip is also shown packaged into a compact module, with the measured noise performance shown at the right. (data courtesy of N. Erickson)

The amplifiers shown in Figure 1 use a combination of technologies. At frequencies below 60 GHz, the best results are using InP discrete HEMT devices fabricated into circuits with “chip and wire “ techniques using separate substrates for impedance matching. TRW and HRL Laboratories, both of which

fabricate excellent low noise devices, support those same devices in Monolithic Millimeter Integrated Circuits (MMICs), in which all major circuit functions are carried out on a single chip. The integration of the chip is compact and simple, requiring an input an output and a few bias wires. All of the critical impedance matching circuitry is on chip, making assembly simple and ripe for mass production.

A 75-110 GHz ultra-low noise amplifier has been developed on TRW's InP HEMT MMIC process (Figure 5). On one of the wafers produced, the typical noise temperature is below 45 K from 80-110 GHz Ref [18]. A single good wafer will produce as much as a thousand amplifiers. Typical wafers produced in this process yield results 45-55 K across the same band. Also shown is the amplifier packaged into a simple housing 1.5 cm long. These units are being used to populate polarimeters on COMPASS and polarimetric arrays for the CAPMAP and AMiBA experiments. The last two experiments along with DASI and CBI configured as polarimeters, are the first in a new generation of CMB experiments to use ten or more pixels for polarization measurement.

### 3.2 MMIC Multichip Modules

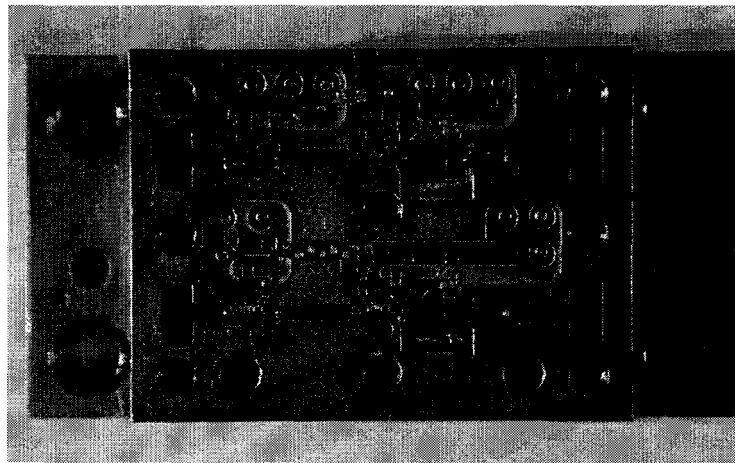


Figure 6. The 100 GHz Planck-LFI breadboard FEM developed by TRW and JPL. The unit is a fully functional pseudocorrelation receiver front end. Three chips are visible in each of two parallel chains comprising two amplification stages and a phase switch. For scale, the four waveguide ports have a large dimension of 0.1 inches.

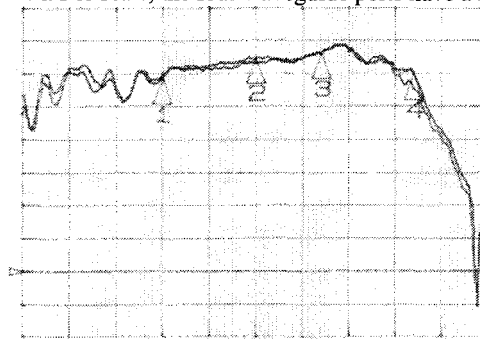


Figure 7. The match of the two channels of the FEM through the couplers. The x-axis is frequency shown from 65-115GHz, The y-axis is gain at 5 dB/div with the reference mark at 0 dB gain. The isolation upon switching is greater than 20 dB across the band.

A great advantage of MMIC integration is the ability to provide multiple radiometer functions in a small space. This is providing new opportunities in dense focal plane arrays and all receivers with a large number of elements.

The first example of a CMB experiment using MMIC multifunction integration, is the Planck-LFI. The Front-End Module (FEM) comprises a waveguide hybrid coupler, two amplifier chains, with phase switches and an output hybrid coupler, all cooled to 22K in a package a few cm on a side. The 100 GHz breadboard version of this module was produced by TRW and JPL, and is shown with the lid off in Figure 6. The amplifiers are the same as those described in the last section. The phase switches were designed and

fabricated by TRW on their InP PIN MMIC process. The swept RF gain in the two channels is shown in Figure 7. The noise performance of this module is 49K from 85-105 GHz. The complete receiver has an instantaneous noise of  $500 \mu\text{K}\sqrt{\text{sec}}$ . This same level of integration can be applied to polarimeter arrays.

#### 4. COHERENT POLARIMETER ARRAYS

Several groups have proposed CMB polarimeter arrays with a large number of elements. The sensitivity one might obtain on a per element basis is  $250 \mu\text{K}\sqrt{\text{sec}}$  at 100 GHz and  $170 \mu\text{K}\sqrt{\text{sec}}$  using today's numbers for amplifier performance. A 100 element array would then achieve a sensitivity of  $25 \mu\text{K}\sqrt{\text{sec}}$ , at 100 GHz. To reach a sensitivity of  $1 \mu\text{K}$  per pixel, an integration time of a day might be required for a 100 pixel map, or 100 days per 10,000 pixel map. These integration times are readily achievable at ground-based sites like Atacama and the South Pole.

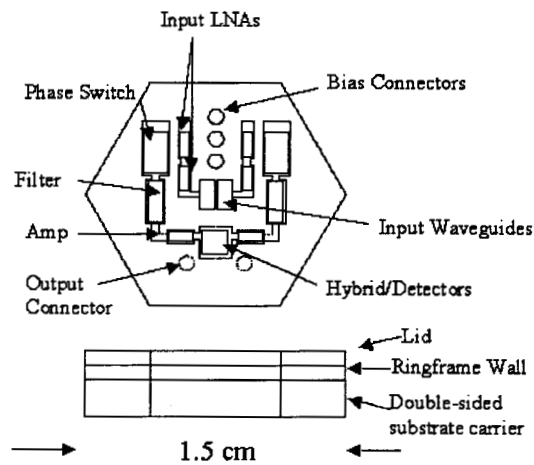


Figure 8. Layout of a 100 GHz polarimeter module for a dense array receiver. The module was designed to use existing chips developed for Planck-LFI.

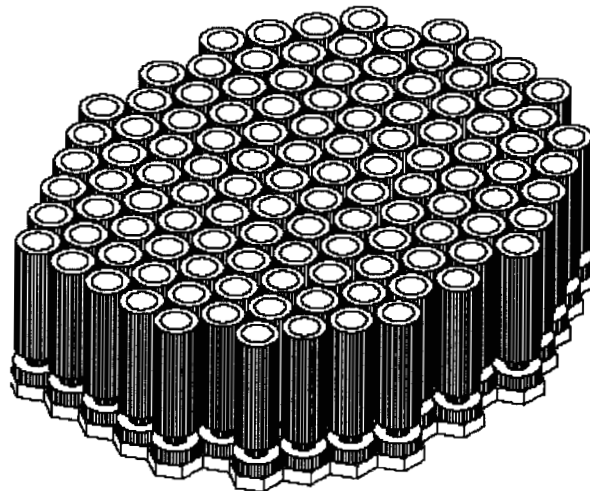


Figure 9. Conceptual drawing of how 100 array elements fit together. The receivers are shown with their feed horns and circular polarizers.

In order to achieve element density and cost savings required to fabricate such an array, mass production techniques would have to be employed. We have found that using existing chips, and double-sided packaging, we can fit a fully functional polarimeter into package the size of a quarter (Figure 8). Questions remain about the difficulty in packing millimeter-wave circuits so tight, module linearity, cooling detector diodes and video amplifiers. For this reason it is anticipated that the first few of these polarimeters may be quite expensive, with the cost dropping to under \$1000, in large quantities, in production. A drawing of this array concept is shown in Figure 9.

Problems not addressed, but common to both coherent and incoherent detectors, is the accommodation of the optical requirements in a large focal plane. Because foregrounds are expected to dominate the CMB B-mode polarization signal, measurements from 30-400 GHz will likely be required. At 30 GHz, the optical problem translates to a large optical system. For this reason, it is well worth considering interferometers as an option. The  $n(n-1)/2$  correlator problem might also be solved using MMIC multichip module technology.

If the science goal for CMB polarization requires full sky or nearly full sky coverage, receiver noise figures must be brought closer to the quantum limit. InP technology has demonstrated the potential to deliver 3 times quantum limited noise or 15 K at 100 GHz. The gain of the current generation of transistors must be increased to realize this goal. Shorter gate lengths and process refinement may yield such results within a decade. In addition new materials are being explored which hold great potential for cryogenic noise performance. TRW and HRL have both been funded under a DARPA program to develop Sb based semiconductors. Device physics models show that if the leakage can be controlled, the devices should offer a factor of two in performance over InP. The development effort has been set up in much the same way as the effort that resulted in InP.

SIS receivers offer an alternative to HEMTs. Above 100 GHz, noise near 3 times the quantum limit has been demonstrated. Increased IF bandwidth, along with better IF amplifiers have made coherent detection competitive Ref[19]. The recent discovery of  $MgB_2$  superconductors, with a  $T_c$  of 39 K, has opened the possibility of SIS receivers at 20K, greatly simplifying the experiment Ref[20].

A receiver with 15K noise at 100 GHz, with 20 GHz bandwidth, configured for Q and U detection, will have an instantaneous sensitivity of  $70 \mu K \sqrt{\text{sec}}$  (in space), a factor of 16 improvement in mapping speed over today's technology.

## 5. SUMMARY AND CONCLUSIONS

Coherent radiometers have demonstrated the ability to make sensitive measurements of the CMB. For ground-based experiments, for the next decade, it is likely that amplifier based receivers will continue to provide state-of-the-art measurements of the CMB. Using dense packaging techniques in multichip-multifunction modules, polarimeter functionality can be assembled into large format arrays.

## ACKNOWLEDGEMENTS

The author would like to thank many individuals who contributed to this work including Mary Wells, and Michael Tsai who worked on the Planck EBB modules, Michael Sholley, Bob Haas, Linda Reed, Bill Brunner, Jack Elderedge, Rich Lai, Ron Grundbacher and Aaron Oki at TRW who have all supported the Planck-LFI effort. The Planck RWG provided constant useful input into the development of compact receivers. Marian Pospieszalski and Niklas Wadefalk provided data on amplifier noise. Finally Charles Lawrence and Mike Seiffert, for many useful discussions on polarimeter design. Portions of this work were carried out at the Jet Propulsion Laboratory, California Institute of Technology, under a contract with the National Aeronautics and Space Administration (NASA). This work was supported by NASA under the Planck LFI program.

## REFERENCES

- [1] B. Netterfield et al., "A measurement by BOOMERANG of multiple peaks in the angular power spectrum of the cosmic microwave background, *Submitted Ap.J. April 2001*
- [2] S. Padin et al, "First intrinsic anisotropy observations with the Cosmic Background Imager", *Ap. J Letters*, 549,L1-L5, March, 2001
- [3] N. W. Halverson et al, "DASI First Results: A measurement of the cosmic microwave background background angular power spectrum", *Ap.J.* 568, p38-45 2002

- [4] C. Bennett, A. Banday, K. Gorski, G. Hinshaw, P. Jackson, P. Keegstra, A. Kogut, G. Smoot, D. Wilkinson, E. Wright, "4-Year COBE DMR Cosmic Microwave Background Observations: Maps and Basic Results", *Ap. J.*, 464, L1-4, 1996
- [5] M. Hedman, D. Barkats, J. Gundersen, J. McMahon, S. Staggs, B. Winstein, "New limits on the polarized anisotropy of the cosmic microwave background at subdegree angular scales", *submitted Ap. J. Lett.*
- [6] W. Hu, M. White, "A CMB Polarization Primer", *New Astronomy*, 2, 323, 1997
- [7] C. Caves, "Quantum limits on noise in linear amplifiers", *Phys Rev D*, 26, p1817, 1982
- [8] J. Webber, M. Pospieszalski, "Microwave instrumentation for radio astronomy", *Microwave Theory and Techniques, IEEE Transactions on*, 50 Issue 3, p 986, March 2002
- [9] J. Kooi, M. Chan, B. Bumble, H. LeDuc, P. Schaffer, T. Phillips, "230 and 492 GHz Low Noise SIS Waveguide Receivers Employing Tuned Nb/AlO<sub>x</sub>/Nb Tunnel Junctions", *Int. J. IR and MM Waves*, 16, 12, 1995
- [10] J. Kraus, *Radio Astronomy*, Cygnus-Quasar Books, 2<sup>nd</sup> Ed., 1980
- [11] R. Dicke, "The measurement of thermal radiation at microwave frequencies", *Rev. Sci. Instr.*, 17, p268, 1946
- [12] P. Lubin, G. Smoot, *Ap J.* 245, 1 1981
- [13] Seiffert et al, "1/f noise and other systematic effects in the Planck-LFI radiometers", *accepted Astron and Astroph*, 2002
- [14] B. Keating, P. Timbie, A. Polnarev, J. Steinberger, "The large scale angular polarization of the cosmic microwave background radiation and the feasibility of its detection", *Ap J.* 495 p580, 1998
- [15] M. Orsini, E. Carretti, S. Cortiglione, "An overview of the SPORt experiment", *Astr and Astroph Trans, Proc Gamov Mem. Intl. Conf*, 19, p 277, St. Petersburg 1999 (2000)
- [16] S. Cortiglione, C. Macculi, "BaR-SPORt Web Page", <http://sport.bo.iasf.cnr.it/Bar/index>
- [17] B. Bennett, "The map web page", <http://map.gsfc.nasa.gov>
- [18] S. Weinreb, R. Lai, N. Erickson, T. Gaier, J. Weilgus, "W-band InP wideband MMIC LNA with 30 K noise temperature", *IEEE-MTT-S Int. Micr Symp Dig.*, 1, p101, 1999
- [19] L. Page, "The MINT Official Web Page", <http://imogen.Princeton.edu/mintweb/>
- [20] J. Nagamatsu, N. Nakagawa, T. Muranaka, Y. Zenitani, J. Akimitsu, "Superconductivity at 39 K in MgB<sub>2</sub>", *Nature*, 410, p63, 2001